

Effect of Charge Status on the Ion Transport and Antimicrobial Activity of Synthetic Channels.

Pengyang Xin,* Lingyu Zhao, Linlin Mao, Linqi Xu, Shuaimin Hou, Huiyuan Kong,
Haodong Fang, Haofeng Zhu, Tao Jiang and Chang-Po Chen*

Henan Key Laboratory of Organic Functional Molecule and Drug Innovation, Key
Laboratory of Green Chemical Media and Reactions of Ministry of Education,
Collaborative Innovation Center of Henan Province for Green Manufacturing of Fine
Chemicals, School of Chemistry and Chemical Engineering, Henan Normal
University, Xinxiang, Henan 453007, China.

*To whom correspondence should be addressed: pyxin27@163.com;
changpochen@yahoo.com.

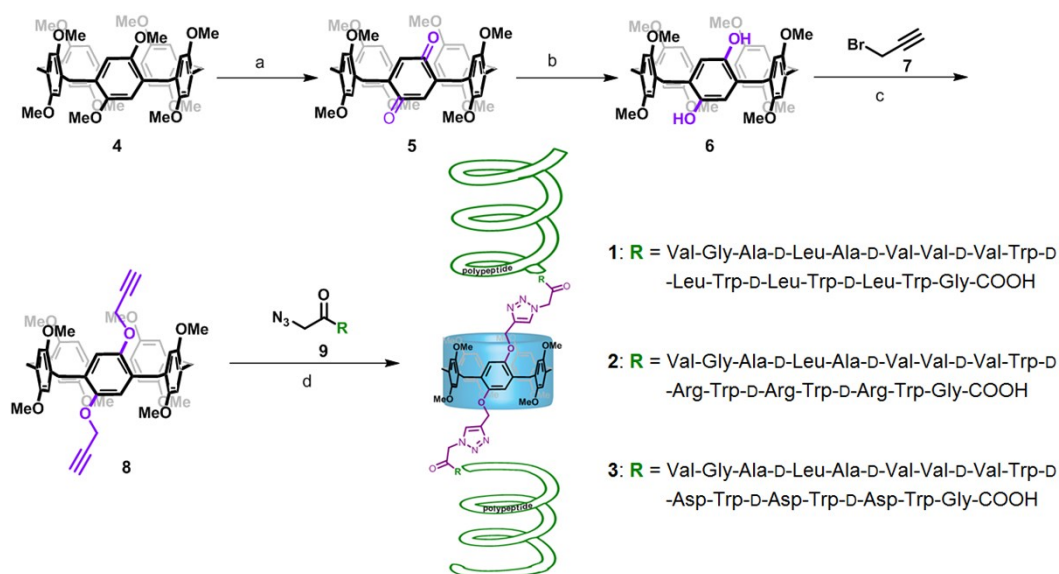
Contents

1. General	S2
2. Synthetic procedures and characterization data for 1-3	S2
3. Procedures for proton transport experiments	S13
4. Procedures for planer lipid bilayer conductance experiments	S14
5. Procedures for the measurement of antimicrobial activity	S17
6. Procedures for the measurement of hemolytic toxicity	S20
7. Molecular modelling studies:	S20
8. References	S21

1. General:

Egg yolk L- α -phosphatidylcholine was obtained from Sigma-Aldrich as ethanol solution (100 mg/mL). 1,2-diphytanoyl-*sn*-glycero-3-phosphocholine (diPhyPC) was obtained from Avanti Polar Lipids as chloroform solution (10 mg/mL). The Fmoc-protected amino acids were obtained from GL Biochem (Shanghai) Ltd. The peptides were synthesized by PTI PS3 automated peptide synthesizer. The ^1H and ^{13}C NMR spectra were recorded on commercial instruments (600 MHz) at 298 K. Chemical shifts were referenced to solvent residue. Mass spectra were recorded with Bruker MicroTOF II spectrometer by using positive or negative mode. The fluorescent experiments on vesicles were performed on Varian Cary Eclipse fluorescence spectrophotometer. The conductance measurement on planar lipid bilayer was performed on Warner BC-535D Planar Lipid Bilayer Workstation.

2. Synthetic procedures and characterization data:



Scheme S1 Synthesis of compounds **1-3**: (a) $(\text{NH}_4)_2\text{Ce}(\text{NO}_3)_6$, DMA/ H_2O , r.t.; (b) NaBH_4 , THF/MeOH, r.t.; (c) K_2CO_3 , CH_3CN , 60°C ; (d) $\text{CuSO}_4 \cdot 5\text{H}_2\text{O}$, Sodium ascorbate, DMSO, r.t.

Compound 5. To a solution of **4**¹ (3.0 g, 4 mmol) in dichloromethane (DCM) (300 mL) was added $(\text{NH}_4)_2\text{Ce}(\text{NO}_3)_6$ (4.38 g, 8 mmol) and water (3 mL).² After addition, the mixture was stirred at room temperature for 10 minutes. Then the mixture was washed with water and the organic solution was dried over anhydrous Na_2SO_4 . After removing of the solvent, the crude product was purified by column chromatography on silica gel to yield **5** as red solid.

5: Yield: 35%. $^1\text{H NMR}$ (CDCl_3 , 600MHz) δ : 6.84(s, 2H), 6.81(s, 2H), 6.79 (s, 2H), 6.67 (s, 2H), 6.66 (s, 2H), 3.79 (s, 6H), 3.74 (s, 6H), 3.71 (s, 12H), 3.63 (s, 6H), 3.59 (s, 4H). HRMS: Calcd for $\text{C}_{43}\text{H}_{44}\text{NaO}_{10}$ $[\text{M}+\text{Na}]^+$: 743.2832. Found: 743.2867.

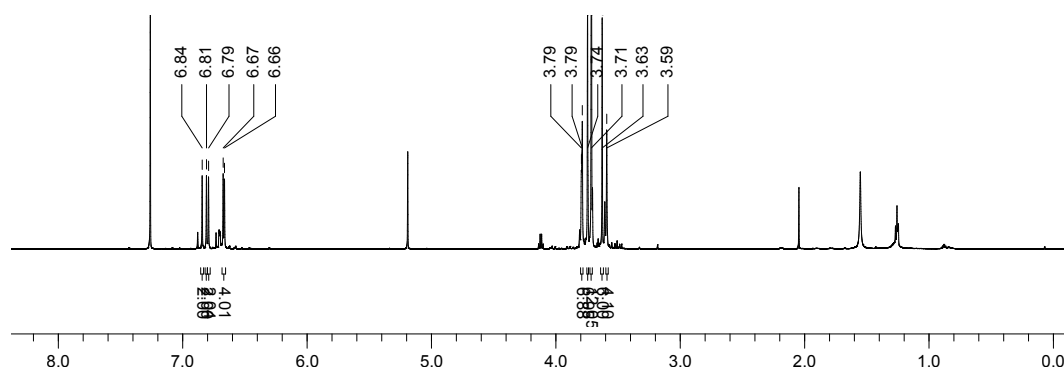


Fig. S1. $^1\text{H NMR}$ spectrum of **5** in CDCl_3 .

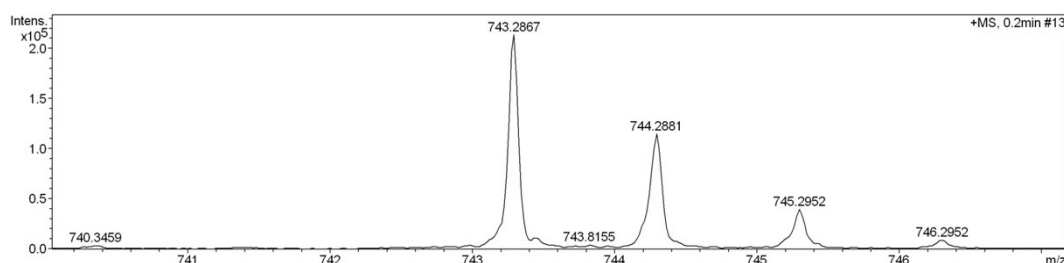


Fig. S2. HR-MS of **5**.

Compound 6. To a solution of **5** (0.5 g, 0.7 mmol) in THF (15 mL) and CH_3OH (5 mL) was added NaBH_4 (0.13 mg, 3.50 mmol).³ The mixture was stirred at room temperature for 30 min. The reaction was quenched by pouring into 0.5 M HCl aqueous solution. Then ethyl acetate and water were added to the mixture. The organic layer was dried over anhydrous Na_2SO_4 . After removing of the solvent, the crude product was purified by column chromatography on silica gel to yield **6** as white solid.

6: Yield: 57%. $^1\text{H NMR}$ ($\text{DMSO}-d_6$, 600MHz) δ : 8.22 (s, 2H), 6.84(s, 2H), 6.83 (s, 2H), 6.79 (s, 2H), 6.78 (s, 2H), 6.54 (s, 2H), 3.71 (s, 6H), 3.68 (s, 6H), 3.65 (s, 12H), 3.63 (s, 6H), 3.55 (s, 4H). HRMS: Calcd for $\text{C}_{43}\text{H}_{46}\text{NaO}_{10}$ $[\text{M}+\text{Na}]^+$: 745.2989. Found: 745.2997.

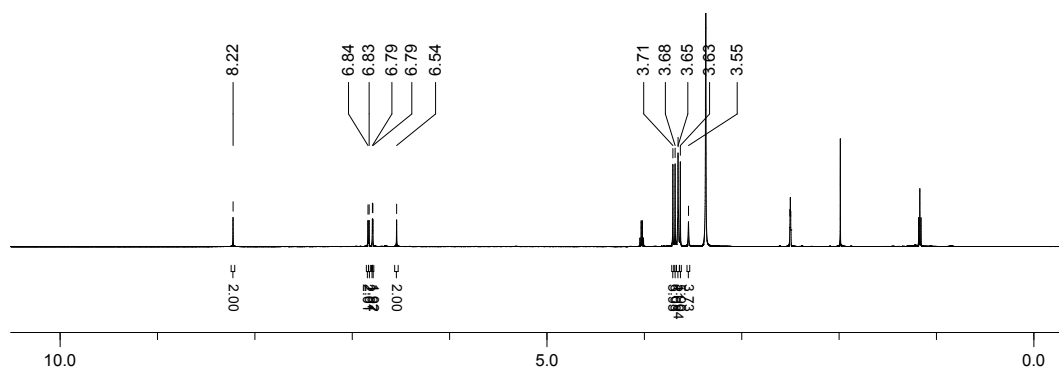


Fig. S3. ^1H NMR spectrum of **6** in CDCl_3 .

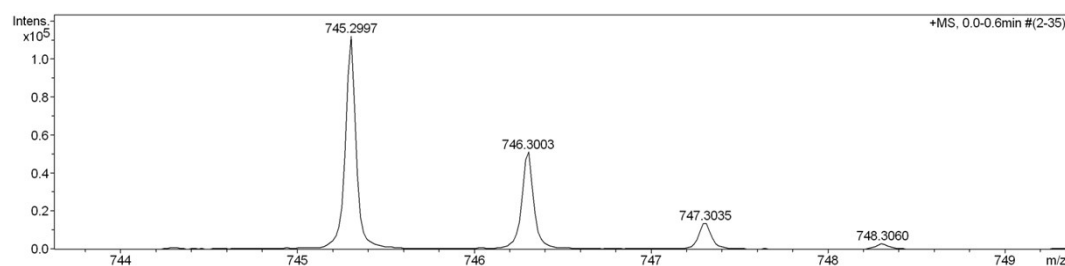


Fig. S4. HR-MS of **6**.

Compound 8. Under a nitrogen atmosphere, **6** (0.2 g, 0.28 mmol) was dissolved in CH_3CN (10 mL). K_2CO_3 (0.6 mg, 1.4 mmol) was added, and the reaction mixture was stirred at $60\text{ }^\circ\text{C}$ for 2 h. Then propargyl bromide **7** (0.17 mL, 2.24 mmol) was added, and the reaction mixture was stirred at $60\text{ }^\circ\text{C}$ for 24 h. After removal of the solvent, the resulting solid was dissolved in ethyl acetate and water. The organic layer was dried over anhydrous Na_2SO_4 . After removing of the solvent, the crude product was purified by column chromatography on silica gel to yield **8** as white solid.

8: Yield: 52%. ^1H NMR (CDCl_3 , 600MHz) δ : 6.79 (s, 2H), 6.78(s, 2H), 6.76 (s, 2H), 6.74 (s, 2H), 6.69 (s, 2H), 4.47 (d, 4H), 3.79-3.77 (br, 10H), 3.68 (s, 6H), 3.66 (s, 6H), 3.62 (d, 12H), 1.94 (br, 2H). ^{13}C NMR (100 MHz, $\text{DMSO}-d_6$) δ 150.3, 150.3, 149.1, 128.4, 128.0, 127.8, 127.7, 127.4, 115.2, 113.7, 113.7, 113.5, 113.5, 80.2, 77.7, 60.2, 56.5, 55.8, 55.7, 55.7, 31.3, 29.5, 29.4, 29.3, 22.3, 21.2, 14.5. HRMS: calcd for $\text{C}_{49}\text{H}_{50}\text{NaO}_{10}$ $[\text{M}+\text{Na}]^+$ 821.3302, found 821.3261.

HRMS: calcd for $C_{100}H_{139}N_{23}O_{18}$ $[M+H]^+$ 1951.0702, found 1951.0801.

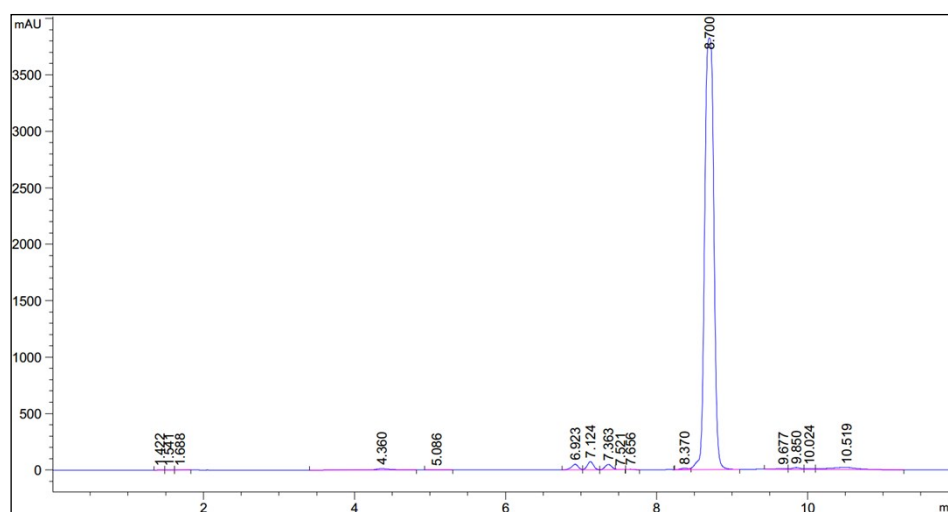


Fig. S8. HPLC analytic trace of **9a**

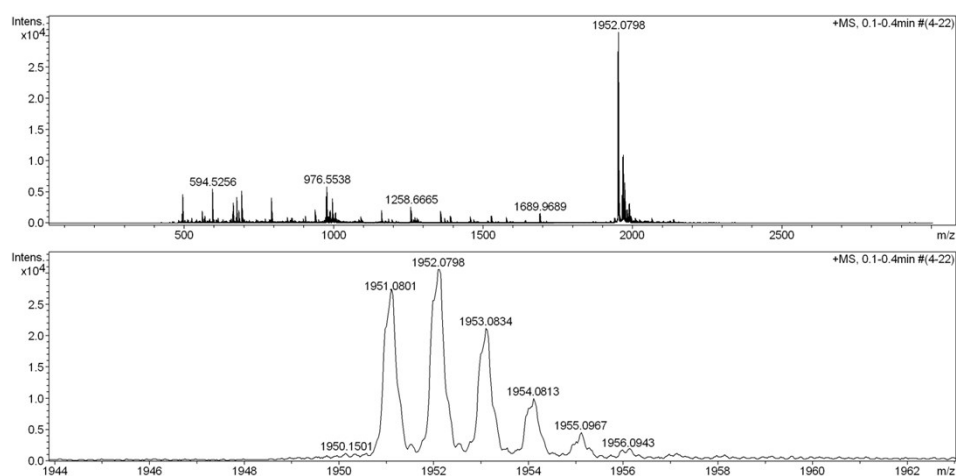


Fig. S9. HR-MS of **9a**.

9b: N_3 -CH₂-CO-Val-Gly-Ala-D-Leu-Ala-D-Val-Val-D-Val-Trp-D-Arg-Trp-D-Arg-Trp-D-Arg-Trp-Gly-COOH

HRMS: calcd for $C_{100}H_{144}N_{32}O_{18}$ $[M+2H]^{2+}$ 1041.0685, found 1041.0771.

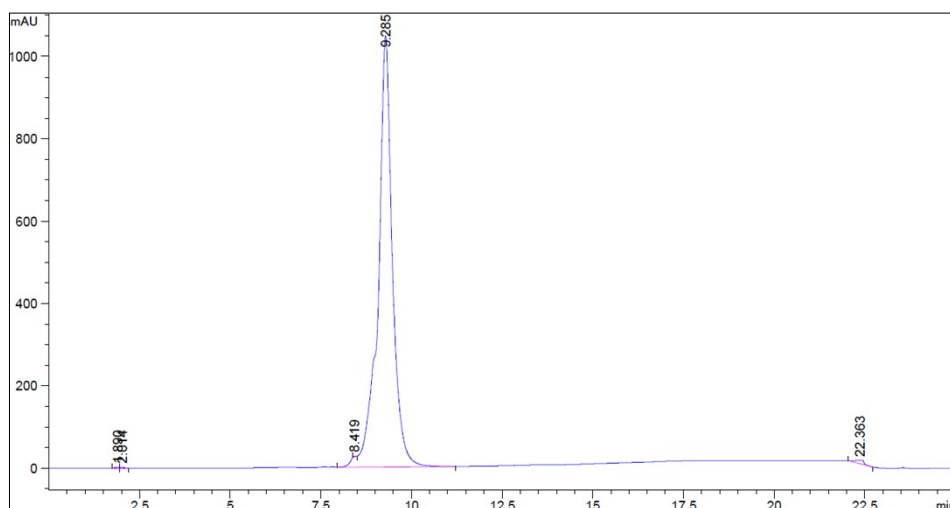


Fig. S10. HPLC analytic trace of **9b**

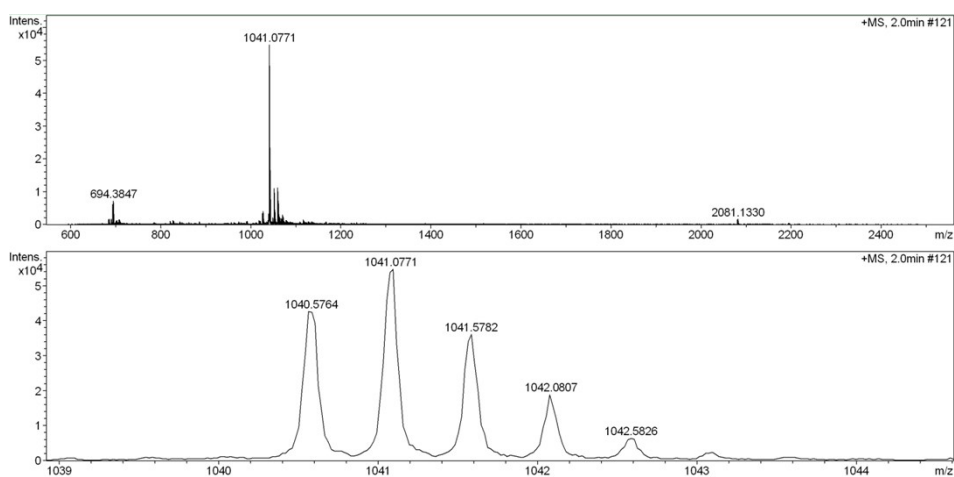


Fig. S11. HR-MS of **9b**.

9c: N₃-CH₂-CO-Val-Gly-Ala-D-Leu-Ala-D-Val-Val-D-Val-Trp-D-Asp-Trp-D-Asp-Trp-D-Asp-Trp-Gly-COOH

HRMS: calcd for C₉₄H₁₂₂KN₂₃O₂₄ [M+K+H]²⁺ 998.4532, found 998.3904.

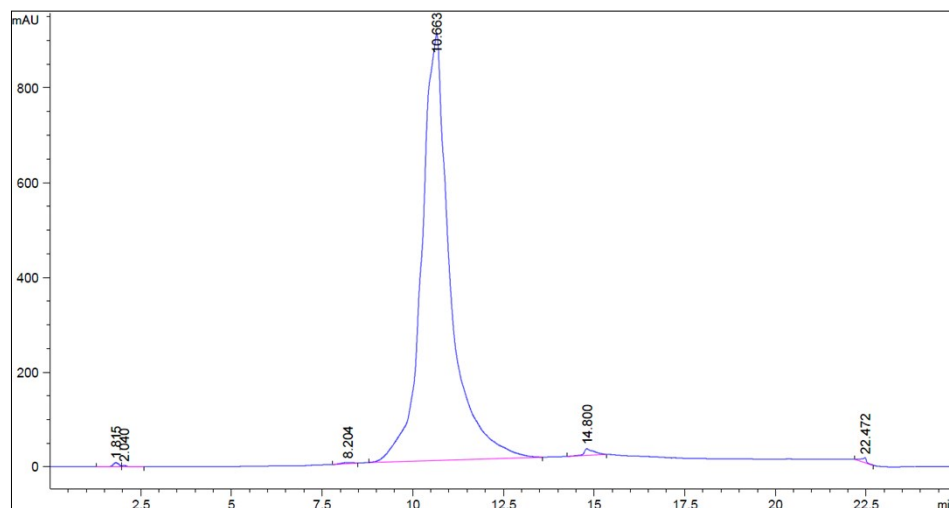


Fig. S12. HPLC analytic trace of **9c**

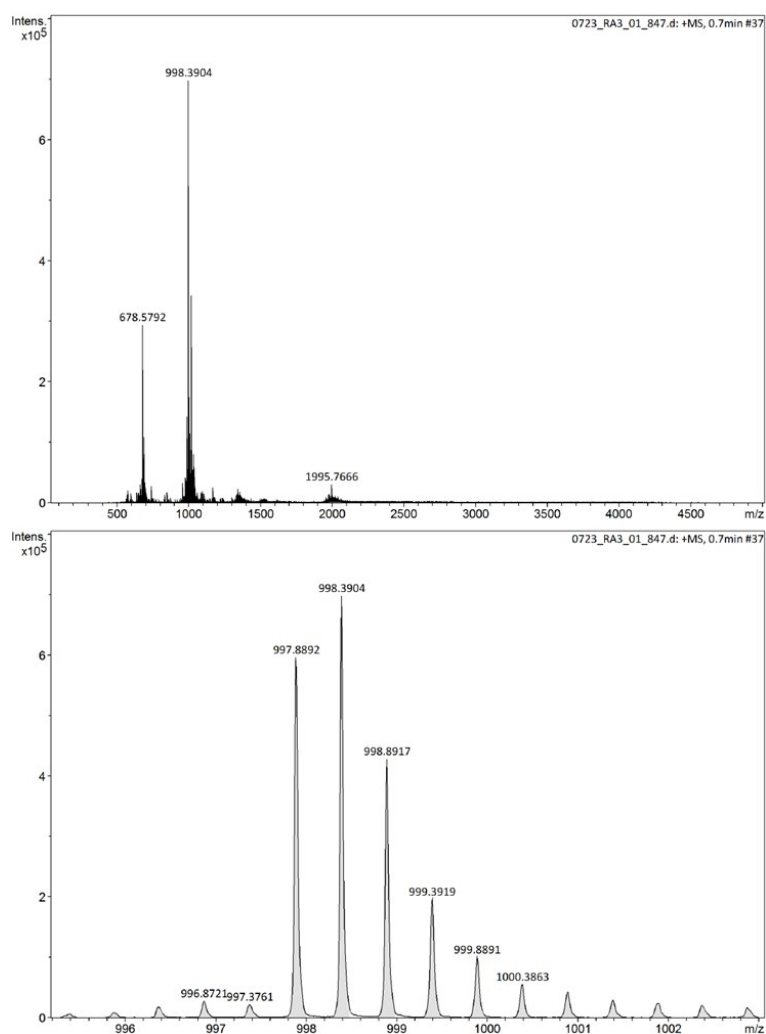


Fig. S13. HR-MS of **9c**.

Compound 1. Compound **9a** (74 mg, 0.075 mmol) was dissolved in DMSO (8 mL).

Fig. S15. ^{13}C NMR spectrum of **1** in $\text{DMSO-}d_6$.

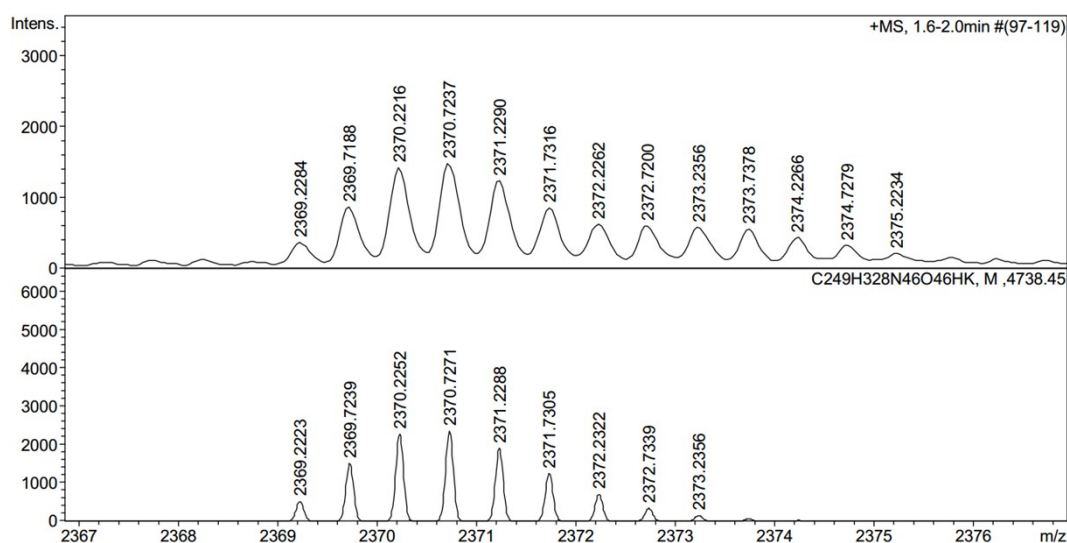


Fig. S16. HR-MS of **1**.

Compound 2. This compound was synthesized from **8** and **9b** according to the same procedure with compound **1**.

2: Yield: 42%. ^1H NMR ($\text{DMSO-}d_6$, 600MHz) δ : 10.56 (br, 2H), 10.69 (s, 2H), 10.66 (s, 6H), 8.52-8.38 (m, 6H), 8.31-8.08 (m, 16), 7.94 (br, 8H), 7.80-7.74 (m, 4H), 7.62-7.57 (d, 8H), 7.35-7.29 (m, 18H), 7.14-6.93 (m, 30H), 6.78-6.74 (m, 10H), 5.26 (q, $J = 12$, 4H), 5.00 (q, $J = 12$, 4H), 4.65-4.58 (m, 8H), 4.29-4.14 (m, 20H), 3.79 (br, 6H), 3.67 (br, 28H), 3.51 (s, 8H), 3.19-3.09 (m, 10H), 2.90-2.81 (m, 18H), 2.06-1.99 (m, 8H), 1.79-1.75 (m, 2H), 1.55 (br, 4H), 1.46 (br, 4H), 1.21-1.15 (m, 32H), 1.06-0.99 (m, 8H), 0.89-0.79 (m, 48H), 0.55-0.51 (m, 12H). ^{13}C NMR (100 MHz, $\text{DMSO-}d_6$) δ 172.8, 172.7, 172.3, 171.9, 171.6, 171.6, 171.5, 171.5, 171.4, 171.4, 171.3, 171.3, 171.2, 171.2, 169.1, 168.9, 166.1, 158.8, 158.6, 157.0, 150.3, 150.3, 149.6, 143.5, 136.5, 136.5, 136.4, 136.4, 136.4, 128.4, 128.0, 127.9, 127.8, 127.8, 127.6, 127.6, 127.5, 126.1, 126.1, 126.0, 124.5, 124.4, 124.4, 124.4, 124.3, 124.3, 121.2, 119.0, 119.0, 119.0, 118.8, 118.8, 118.7, 118.6, 118.6, 118.6, 118.5, 116.7, 115.0, 114.9, 113.8, 113.8, 113.7, 113.7, 111.7, 111.6, 111.6, 110.3, 110.2, 110.1, 110.1, 62.2, 58.5, 58.2, 58.2, 57.9, 55.9, 55.8, 52.4, 52.4, 51.9, 51.9, 51.7, 49.1, 49.1, 49.0, 46.2, 42.2, 41.2, 41.0, 40.9, 40.9, 40.6, 40.5, 31.2, 31.1, 31.0, 29.6, 29.6, 29.5, 29.5, 29.4, 29.4, 29.3, 29.3, 29.3, 29.2, 29.2, 29.0, 28.8, 28.6, 27.0, 25.6, 24.8, 24.7, 23.4, 22.5, 21.6, 19.7, 19.7, 19.6, 19.5, 18.7, 18.5, 18.4, 18.1, 17.9, 17.9, 14.4, 9.1, 0.6. HRMS: calcd for $\text{C}_{249}\text{H}_{338}\text{N}_{64}\text{O}_{46} [\text{M}+4\text{H}]^{4+}$ 1240.6536, found 1240.6493.

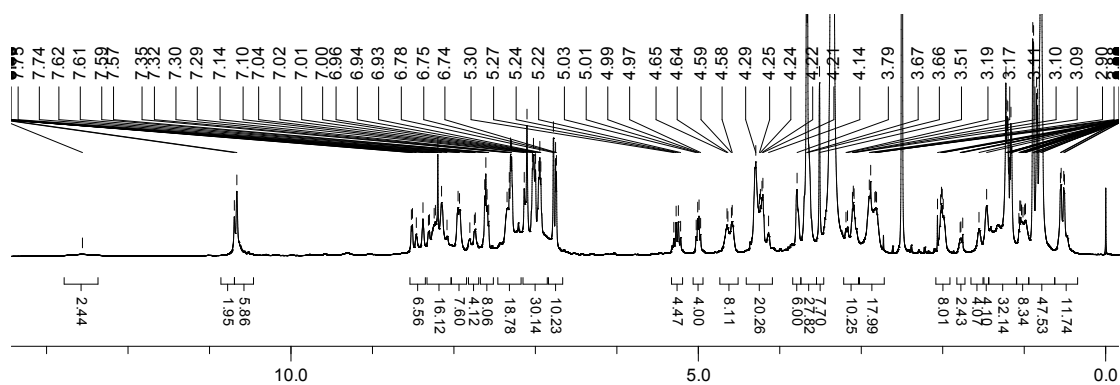


Fig. S17. ^1H NMR spectrum of **2** in $\text{DMSO-}d_6$.

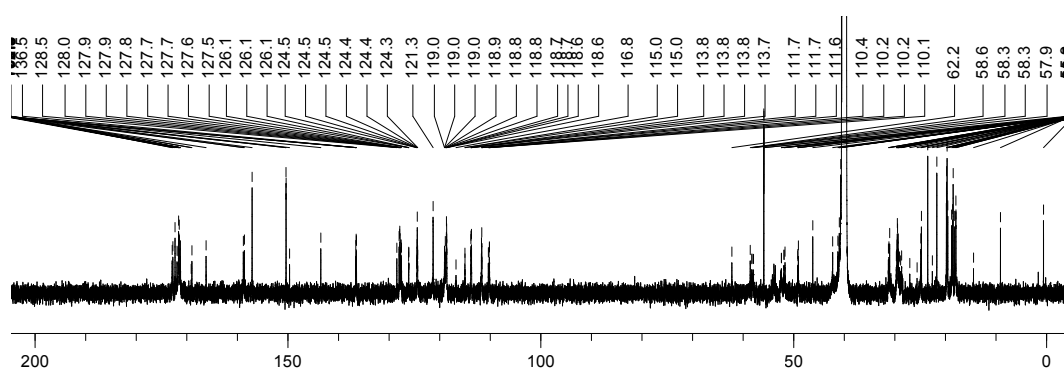


Fig. S18. ^{13}C NMR spectrum of **2** in $\text{DMSO-}d_6$.

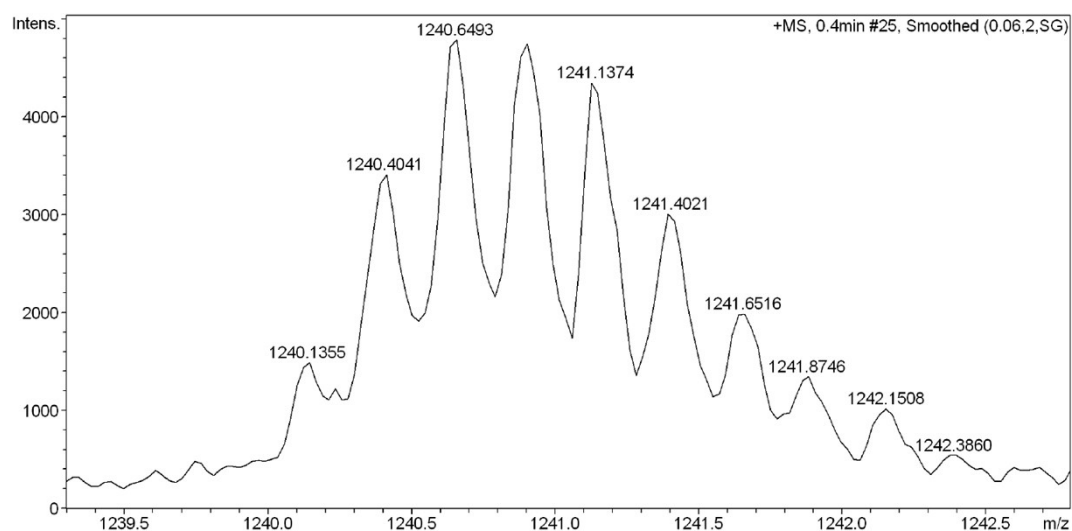


Fig. S19. HR-MS of **2**.

Compound 3. This compound was synthesized from **8** and **9c** according to the same procedure with compound **1**.

3: Yield: 52%. ^1H NMR ($\text{DMSO-}d_6$, 600MHz) δ : 12.33 (br, 8H), 10.74 (s, 2H), 10.69 (s, 4H), 10.64 (s, 2H), 8.51 (d, $J = 6$, 2H), 8.37 (br, 6H), 8.30-8.27 (m, 4H), 8.19 (s, 2H), 8.14-8.10 (m, 4H), 8.01-7.90 (m, 12H), 7.82-7.74 (m, 4H), 7.60-7.54

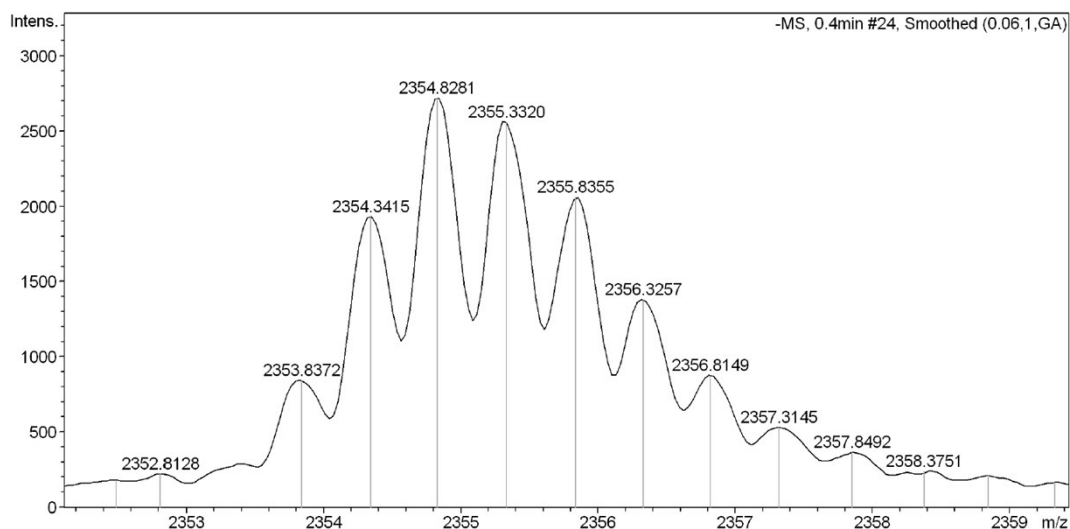


Fig. S22. HR-MS of **3**.

3. Procedures for proton transport experiments:⁴

Preparation of HPTS containing large unilamellar vesicles (LUVs): EYPC (15 mg, 20 μmol) in EtOH (0.15 mL) was diluted with EtOH (5.0 mL), the solution was evaporated under reduced pressure, and the resulting thin film was dried under high vacuum for 3 h. The lipid film was hydrated with HEPES buffer solution (1.5 mL, HEPES (10 mM), KCl (100 mM), pH = 7.2) containing HPTS (0.1 mM) at 40 $^{\circ}\text{C}$ for 2 h to give a milky suspension. The resulting suspension was subjected to ten freeze-thaw cycles by using liquid N_2 to freeze and warm water bath to thaw. The suspension was dialyzed with membrane tube (MWCO = 14000) against the same HEPES buffer solution (200 mL, without HPTS) for six times to remove un-entrapped HPTS and produce vesicle suspension ($[\text{lipid}] = 13.3 \text{ mM}$).

Fluorescent experiments: HEPES buffer solution (2.0 mL, HEPES (10 mM), KCl (100 mM), pH = 6.0) and the prepared vesicle suspension (13.3 mM, 100 μL) were placed in a fluorimetric cuvette. To the cuvette, the solution of compound **1-3** in DMSO (5 μL) was added to reach a required channel concentration (molar ratio relative to lipid, represented by x) with gentle stirring. Fluorescent intensity (I_t) was continuously monitored at 510 nm (excitation at 460 nm) in 10 min. Then, Triton aqueous solution (50%, 10 μL) was added with gentle stirring. The intensity was monitored until the fluorescent intensity (I_{∞}) did not change. The collected data were then normalized into the fractional change in fluorescence given by $(I_t - I_0)/(I_{\infty} - I_0)$, where I_0 is the initial intensity.

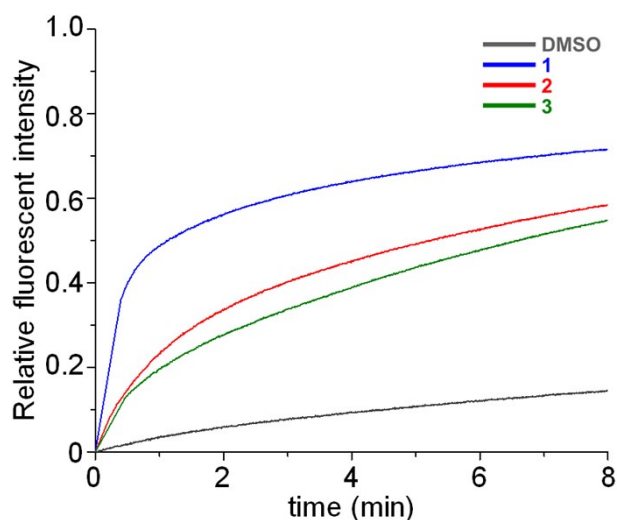


Fig. S23. Changes in the fluorescence intensity of HPTS ($\lambda_{\text{ex}} = 460 \text{ nm}$, $\lambda_{\text{em}} = 510 \text{ nm}$) in vesicles with time after the addition of compounds **1-3** ($x = 0.4\%$, molar ratio relative to lipid, represented by x).

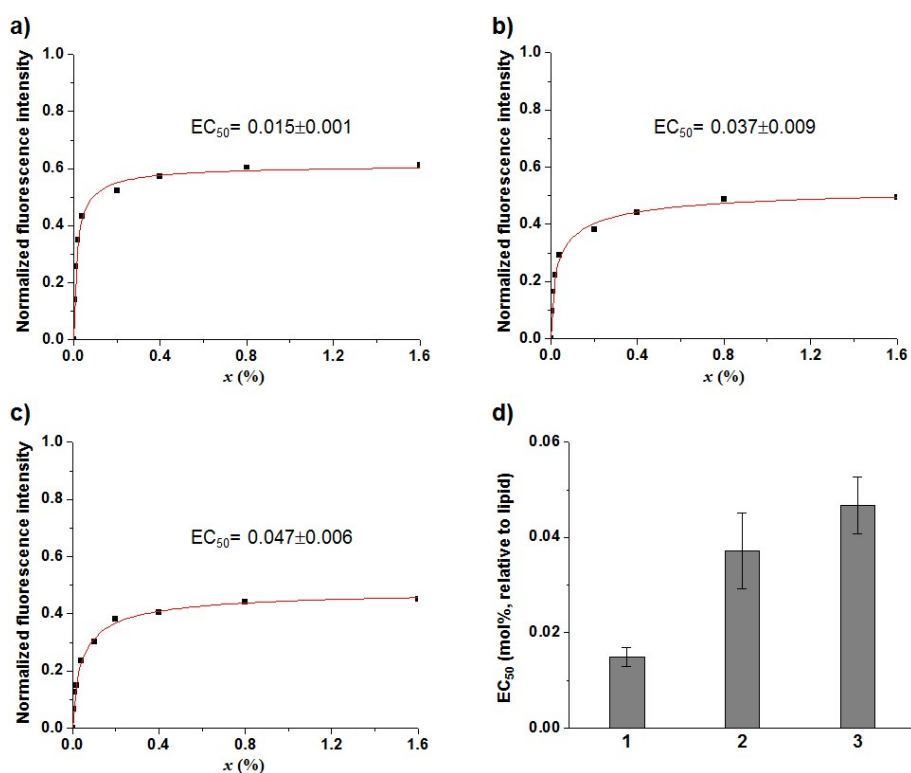


Fig. S24. Changes in normalized fluorescent intensity of HPTS ($\lambda_{\text{ex}} = 460 \text{ nm}$, $\lambda_{\text{em}} = 510 \text{ nm}$) in vesicles with the concentration (molar ratio relative to lipid, represented by x) of **1** (a), **2** (b) and **3** (c). Effective concentration needed for 50% activity (EC_{50}) of **1-3** (d).

4. Procedures for planer lipid bilayer conductance experiments:⁵

The solution of diPhyPC in chloroform (10 mg/ml, 20 μ L) was evaporated with nitrogen gas to form a thin film and re-dissolved in *n*-decane (5 μ L). The lipid solution (0.5 μ L) was injected on to the aperture (diameter = 200 μ m) of the Delrin® cup (Warner Instruments, Hamden, CT) and then evaporated with nitrogen gas. In a typical experiment for measurement of the channel conductance for K⁺, the chamber (*trans* side) and the Delrin cup (*cis* side) were filled with aqueous KCl solution (1.0 M, 1.0 mL). Ag-AgCl electrodes were applied directly to the two solutions and the *cis* one was grounded. Planar lipid bilayer was formed by painting the lipids solution (1.0 μ L) around the pretreated aperture and by judgment of capacitance (80-120 pF). Membrane currents were measured using a Warner BC-535D bilayer clamp amplifier and were collected by PatchMaster (HEKA) with sample interval at 5 kHz and then filtered with a 8-pole Bessel filter at 1 kHz (HEKA). The data were analyzed by FitMaster (HEKA) with a digital filter at 100 Hz.

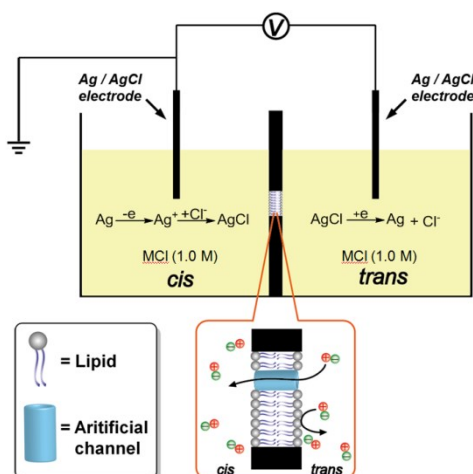


Fig. S25. Schematic representation for the patch clamp experiments with planar lipid bilayer. The redox reactions on both Ag/AgCl electrodes are inserted to illustrate the nature of charge balance during M⁺ transmembrane transport.

For the single-channel conductance measurement, two chambers were charged with KCl (1 M, 1 mL). And the solution of compound **1-3** in DMSO (1 mM, 0.2 μ L) was added to the *trans* compartment and the solution was stirred for 5 min.

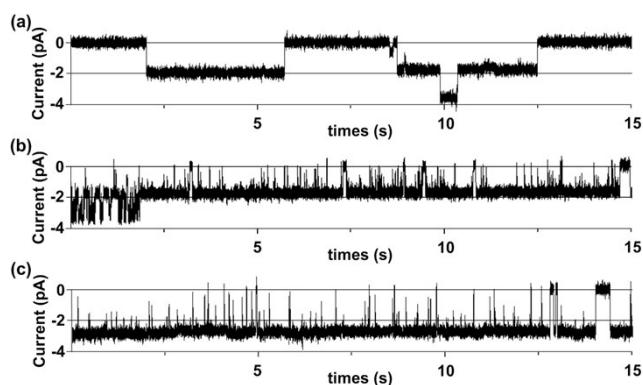


Fig. S26. Current traces through diPhyPC lipid bilayer in 1.0 M KCl at a potential of -80 mV in the presence of 0.2 μ M (a) **1**, (b) **2**, and (c) **3**.

For the measurement of the transport selectivity of K^+ over Cl^- , the KCl solutions (0.2M and 1M) were added to the both side of the bilayer (diPhyPC), *cis* chamber: KCl (1.0 M), *trans* chamber: KCl (0.2 M). The solution of compound **1-3** in DMSO (1 mM, 0.2 μ L) was added to the *trans* compartment and the solution was stirred for 5 min. The permeability (P) ratios of **1-3** for K^+ and Cl^- were calculated according to the Goldman–Hodgkin–Katz equation, and the P_{K^+}/P_{Cl^-} values were determined to be 9.7 (**1**), 2.0 (**2**) and 16.7 (**3**). The high K^+ transport selectivity of **1** may be due in part to its gA-analogous peptidic moieties, which have a suitable cavity to coordinate with dehydrated cations.¹¹ In addition to the similar peptidic moieties, **3** possesses multiple aspartic acid residues at the openings of the channel, which gave channel **3** higher affinity for K^+ ions and resulted in the highest K^+/Cl^- selectivity. The lowest selectivity for K^+/Cl^- of channel **2** might be rationalized by considering that the multiple arginine residues created two positively charged openings, which offer an electrostatic barrier to the entry of K^+ ions into the channel pore.

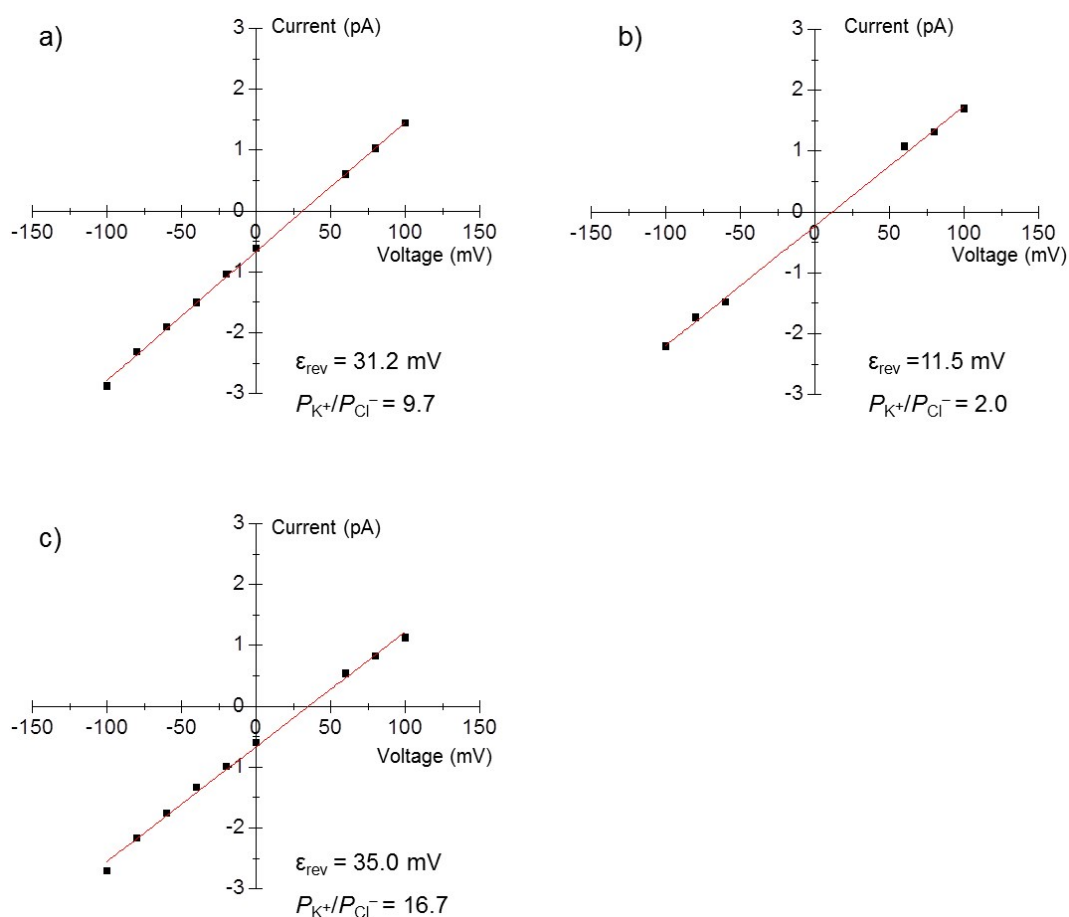


Fig. S27. I - V plots of **1-5** by using unsymmetrical solution at both side of the bilayer. *cis* chamber: KCl (1.0 M), *trans* chamber: KCl (0.2 M). (a) **1**, (b) **2** and (c) **3**.

5. Procedures for the measurement of antimicrobial activity:

(1) Half maximal inhibitory concentrations (IC_{50}):⁶ *B. subtilis* (ATCC 6633), *S. aureus* (ATCC 25923) and *E. coli* (BL21) from a single colony were grown overnight in LB broth at 37 °C with agitation. An aliquot was taken and diluted in fresh broth and cultured until the bacteria reach mid-logarithmic phase ($OD_{595} \approx 0.5$). The bacteria were diluted to a concentration of 5×10^5 CFU/mL. Then, 200 μ L bacterial suspension was added to each well of a sterile 96-well plate. 2.5 μ L DMSO solutions of serial dilution of the channels were added to the wells in triplicates. The plates were shaken for 30 seconds and then incubated at 37 °C overnight before the absorbance at 595 nm was monitored using a microtiter plate reader. The antimicrobial activities of the channels were normalized as bacteria survival (%) = $(OD_{sample+bac} - OD_{broth\ only}) / (OD_{DMSO+bac} - OD_{broth\ only}) \times 100\%$. The channel concentration required to inhibit 50% bacteria growth (IC_{50}) was read out directly from the graph.

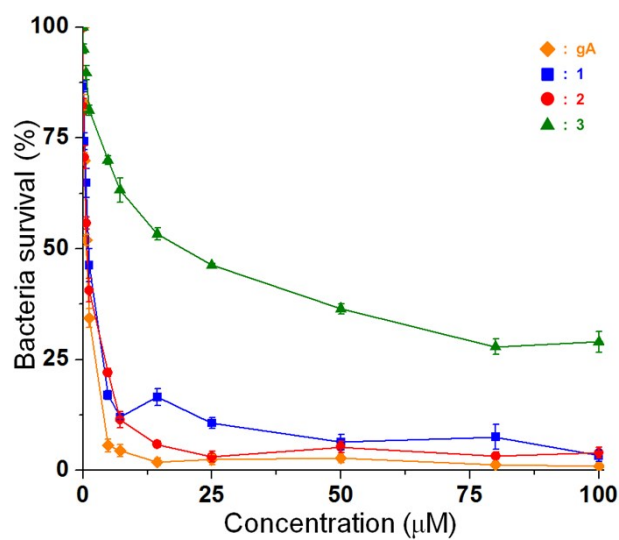


Fig. S28. Antimicrobial activity of 1-3 and gA against Gram-positive bacteria *B.subtilis*.

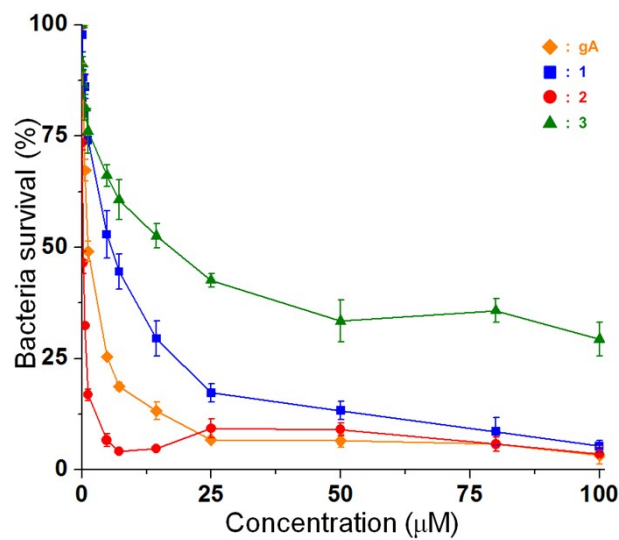


Fig. S29. Antimicrobial activity of 1-3 and gA against Gram-positive bacteria *S.aureus*.

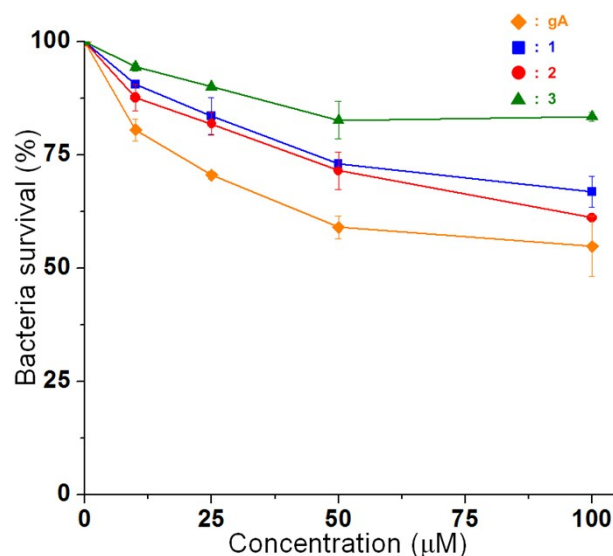


Fig. S30. Antimicrobial activity of **1-3** and gA against Gram-negative bacteria *E. coli*.

(2) Minimal Inhibitory Concentration Measurements (MICs):⁷ MICs were measured against gram-positive *B.subtilis* (ATCC6633), *S.aureus* (ATCC 25923) using the broth microdilution method. The cells were prepared according to the above procedure (Section 5.1). Then, 100 µL bacterial suspension was added to each well of a sterile 96-well plate. 2 µL DMSO solutions of serial dilution of the compounds **1-3** were added to the wells. The plates were shaken for 30 seconds and then incubated at 37 °C overnight. The MIC were readed from the the endpoint as the lowest concentration of compounds **1-3** at which there is no vivible growth.

(3) Solubility test:⁶ The solubility of compounds **1-3** in 10 mM HEPES buffer with 1% DMSO was measured by standard curve method. Briefly, standard curves were obtained from the plots of the absorbance intensity of compounds **1-3** at 280 nm against the concentrations. Then, the concentrated stock solution of **1-3** in DMSO was diluted 100 times (4 µL of the stock into 400 µL of 10 mM HEPES buffer). The mixture was sonicated for 15 mins and then subject to centrifugation (14,000 rpm, 10 mins) to remove possible precipitate. The supernatant (300µL) was transferred to a quartz cuvette and the absorbance intensity was determined at 280 nm. The standard curves and the UV/Vis spectra of saturated solutions of compounds **1-3** can be seen in Figure S30. Extrapolating standard curve by using the absorbance intensity of saturated solutions of 1-3, their solubility were determined to be 74 µg/mL (15.7 µM), 323 µg/mL (65.2 µM) and 226 µg/mL (48.1 µM).

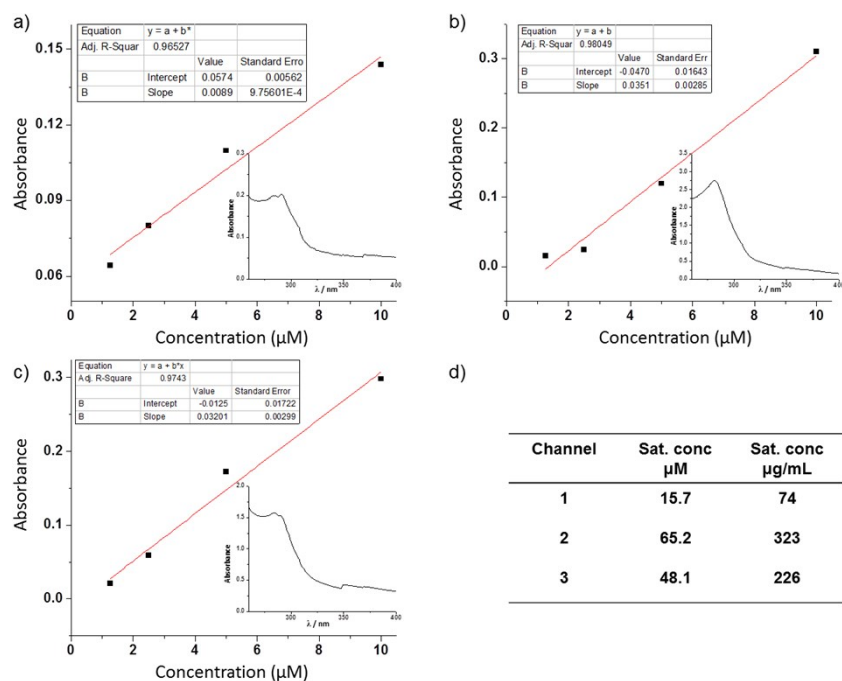


Fig. S31. The standard curve and the UV/Vis spectra of saturated solution of compounds **1** (a), **2** (b) and **3** (c). (d) The solubility of compounds **1-3** in 10 mM HEPES buffer with 1% DMSO.

6. Procedures for the measurement of hemolytic toxicity:⁶

The hemolytic activity of the channels was determined using rat red blood cells (rRBCs). The rRBCs were isolated from fresh Sprague Dawley rat blood by centrifugation at 3500 rpm for 5 min and then washed with PBS buffer until the supernatant was clear. The rRBCs were then resuspended and diluted to a final concentration of 1% (v/v) in PBS and used immediately. To each well of sterile 96-well plate, 200 μL of the erythrocytes suspension were added. And then 2.5 μL of serial dilution of channels in DMSO or DMSO alone were added to the wells in triplicates to reach the required concentration. The plate was gently shaken and then incubated at 37 $^{\circ}\text{C}$ for 30 min, followed by centrifugation at 3500 rpm for 10 min. Aliquots (50 μL) of the supernatant were transferred into a new sterile 96-well plate containing 50 μL of PBS buffer in each well, and the absorbance was measured at 562 nm by a microtiter plate reader. The Percentage hemolysis was calculated as follows: $(A_{\text{sample}} - A_{\text{DMSO}}) / (A_{\text{triton X-100}} - A_{\text{DMSO}}) \times 100\%$. The complete hemolysis was achieved by mixing the erythrocytes with 1% Triton X-100. The channel concentration required to cause 50% hemolysis (HC_{50}) was read out directly from the graph.

7. Molecular modelling studies:

The initial conformation of the helical dimer of gramicidin A and 1,4-

dimethoxypillar[5]arene were taken from the PDB database (PDB ID: 1MAG)⁸ and experimental X-ray crystallographic data,⁹ respectively. A pre-equilibrated DMPC bilayer with 128 lipids was downloaded from CHARMM-GUI.¹⁰

The 1,4-dimethoxypillar[5]arene and gA-analogous peptides were connected by linkers and then minimized to obtain a reasonable model for the channel **2** (Fig. S31a). Then, the optimized tubular model was inserted into a pre-equilibrated DMPC bilayer with 128 lipids, and the lipids overlapping compound **2** were removed. The estimated length of compound **2** from molecular modelling is 4.0 nm. The results indicated that the Arg residuals in the peptide domain of compound **2** were positioned at the headgroup region of lipid bilayer (Fig. S31b). It means that the hydrophilic Arg residuals in the peptide domain of compound **2** were mainly located in the hydrophilic part rather than the hydrophobic domain of lipid bilayers. Therefore, the Arg residuals in the peptide domain of compound **2** might not affect its channel form.

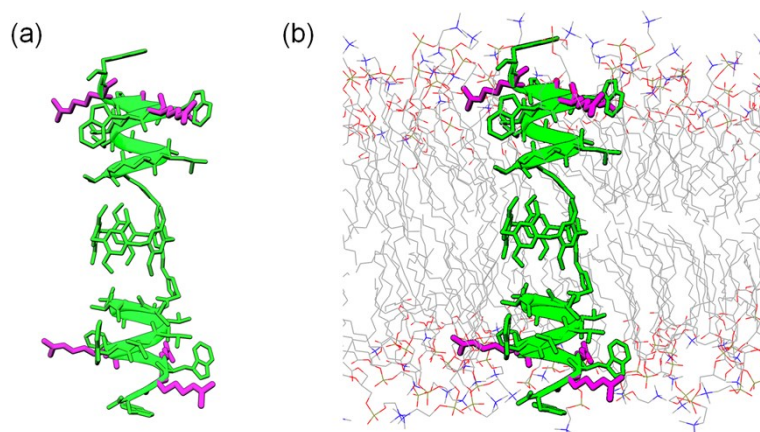


Fig. S32. (a) Side view of the optimized structures of channel **2** and (b) Side view of the equilibrated channel **2**–DMPC system. The Arg residues in the peptide domain of compound **2** were shown in purple.

8. References:

- 1 T. Ogoshi, S. Kanai, S. Fujinami, T. -A. Yamagishi, Y. Nakamoto, *J. Am. Chem. Soc.*, 2008, **130**, 5022.
- 2 C. Han, Z. Zhang, G. Yu, F. Huang, *Chem. Commun.*, 2012, **48**, 9876.
- 3 T. Ogoshi, D. Yamafuji, D. Kotera, T. Aoki, S. Fujinami, T. -A. Yamagishi, *J. Org. Chem.*, 2012, **77**, 11146.
- 4 X.-B. Hu, Z. Chen, G. Tang, J.-L. Hou, Z.-T. Li, *J. Am. Chem. Soc.*, 2012, **134**, 8384.
- 5 R. H. Ashley, *Ion Channels: A Practical Approach*, Oxford University Press, Oxford, U.K., 1995.

- 6 F. Wang, L. Qin, C. J. Pace, P. Wong, R. Malonis, J. Gao, *ChemBioChem*, 2012, **13**, 51.
- 7 J. M. Andrews, *J. Antimicrob. Chemoth.*, 2001, **48**, *Suppl. S1*, 5.
- 8 R. R. Ketchem, K. C. Lee, S. Huo, T. A. Cross, *J. Biomol. NMR*, 1996, **8**, 1.
- 9 T. Ogoshi, S. Kanai, S. Fujinami, T.-A. Yamagishi, Y. Nakamoto, *J. Am. Chem. Soc.*, 2008, **130**, 5022.
- 10 S. Jo, T. Kim, W. Im, *PLOS ONE*, 2007, **2**, e880.